AFRL-RD-TP-
PS-2009-1025

USE OF MULTIPLE CD MAGNETRON DEPOSITION SOURCES FOR UNIFORM COATING OF LARGE AREAS (Preprint)

Stanley Z. Peplinski et al.

S Systems Corporation
PO BOX 9316
Albuquerque NM, 87117

1 June 2009

Technical Paper

AIR FORCE RESEARCH LABORATORY
Directed Energy Directorate
3550 Aberdeen Ave SE
AIR FORCE MATERIEL COMMAND
KIRTLAND AIR FORCE BASE, NM 87117-5776

REPORT DOCUMENTATION PAGE

Form Approved
OMB No. 0704-0188

1. REPORT DATE *(DD-MM-YYYY)*	2. REPORT TYPE	3. DATES COVERED *(From - To)*
01-06-2009	Technical Paper	1 June 2005- 1 June 2009

4. TITLE AND SUBTITLE

Use of multiple DC magnetron deposition sources for uniform coating of large areas (Preprint)

5a. CONTRACT NUMBER
FA9451-04-C-0067 DF297548

5b. GRANT NUMBER

5c. PROGRAM ELEMENT NUMBER
63883C

6. AUTHOR(S)

David W. Reicher, Roberto Christian, Patrick Davidson, Stanley Z. Peplinski

5d. PROJECT NUMBER
5096

5e. TASK NUMBER
SP

5f. WORK UNIT NUMBER
AJ

7. PERFORMING ORGANIZATION NAME(S) AND ADDRESS(ES)

S. Systems Corporation
PO Box 9316
Albuquerque, NM 87117

8. PERFORMING ORGANIZATION REPORT NUMBER

9. SPONSORING / MONITORING AGENCY NAME(S) AND ADDRESS(ES)

Air Force Research Laboratory
3550 Aberdeen Ave SE
Kirtland AFB NM 87117-5776

10. SPONSOR/MONITOR'S ACRONYM(S)
AFRL/RDSO

11. SPONSOR/MONITOR'S REPORT NUMBER(S)
AFRL-RD-PS-TP-2009- 1025

12. DISTRIBUTION / AVAILABILITY STATEMENT

Approved for public release

13. SUPPLEMENTARY NOTES PA approval 377ABW-2009-0831 dtd 30 Jun 09
Accepted for publication in the Thin Film Solar Technology Proceedings, SPIE, Vol. 7409; 04 Sep 2009. "Government Purpose Rights"

14. ABSTRACT

Uniform coating of large areas is a technically challenging aspect of physical vapor deposition This investigation shows that good film uniformity across large areas can be repetitively achieved by a DC magnetron sputtering process by use of multiple sources. A unique feature of this technique is the ability to predict and control the film distribution using the deposition rate, adding flexibility to the deposition system. A model for predicting the material distribution from multiple sources is presented. It will also be demonstrated that this process yields efficient use of the vapor generated from the sources, which results in higher deposition rate and less system maintenance.

15. SUBJECT TERMS
Optical Coatings; Film Uniformity; DC Magnetron Sputtering; Niobium Pentoxide; Silicon Dioxide

16. SECURITY CLASSIFICATION OF:			17. LIMITATION OF ABSTRACT	18. NUMBER OF PAGES	19a. NAME OF RESPONSIBLE PERSON
					Stanley Peplinski
a. REPORT	b. ABSTRACT	c. THIS PAGE			19b. TELEPHONE NUMBER *(include area code)*
Unclassified	Unclassified	Unclassified	SAR	14	505- 846-4197

Standard Form 298 (Rev. 8-98)
Prescribed by ANSI Std. 239.18

Use of multiple DC magnetron deposition sources for uniform coating of large areas

David W. Reicher[a], Roberto Christian[a], Patrick Davidson[a], Stanley Z. Peplinski[b]
[a]S.Systems Corp. PO Box 9316, Albuquerque, NM, USA 87117
[b]AFRL/RDSO 3550 Aberdeen Ave. SE Kirtland AFB, NM, USA 87117-5776

Abstract

Uniform coating of large areas is a technically challenging aspect of physical vapor deposition. This investigation shows that good film uniformity across large areas can be repetitively achieved by a DC magnetron sputtering process by use of multiple sources. A unique feature of this technique is the ability to predict and control the film distribution using the deposition rate, adding flexibility to the deposition system. A model for predicting the material distribution from multiple sources is presented. It will also be demonstrated that this process yields efficient use of the vapor generated from the sources, which results in higher deposition rates and less system maintenance.

Keywords: Optical coatings, film uniformity, DC magnetron sputtering, niobium pentoxide, silicon dioxide

1. Introduction

The distribution of material across a substrate located at some distance from a vapor source has been analyzed for most common vacuum chamber geometries, including simple rotation of a substrate about an axis and planetary rotation.[1,2,3] Most of the investigations have been conducted using evaporation sources, but it has been shown that the same analysis can be applied to magnetron sources.[4,5] Depositing uniform films across the functional region of a substrate is critical in many applications. Non-uniformities in optical coatings create shifts in the spectral characteristics of the coating, in the phase of the reflected and transmitted light and in the mechanical properties of the coating. Depending on the application, film uniformity deviations of less than 0.1% m^{-1} may be required.

Deposition uniformity is usually controlled by the geometry of the source relative to the substrate with in some cases shields interposed between the source and substrate for additional control.[1,3] A method for obtaining deposition uniformity that has been less utilized is multiple sources operating simultaneously, each located at unique distances from the substrate plane. The film distribution resulting from several sources operating simultaneously is the superposition of the distributions from each individual source if the mean free path of the vapor molecules exceeds the source-to-substrate distance. In addition to the location of the sources, the rate of vapor generation from each source may be individually set to further control film distribution. Although this method introduces some operational complications, it has the advantages of added flexibility and improved utilization of the deposition material.

The reactive DC magnetron sputtering process was chosen for this investigation because it produces a vapor plume that changes gradually and predictably as the target erodes and the deposition rate can be controlled accurately by the values of the deposition parameters. In the model and the experiment the substrate surface is rotated at a constant rate with the sources stationary. This leads to a film with uniform azimuthal distribution so that radial distribution is the quantity of interest in this investigation. We define the radial uniformity as the film thickness across the radius normalized to a single point on the radius. Magnetron voltage is the primary means of controlling deposition rate while controlling the argon gas flow rate is secondary. In this investigation six 20cm diameter magnetrons were installed in a 2.5 meter box coater. Each of the magnetrons was powered independently. Results are reported for two materials, SiO_2 deposited from silicon targets and Nb_2O_5 from niobium targets. For each film material three magnetrons were run simultaneously to deposit a uniform layer of material across a 68cm radius, which is the practical limit of the chamber geometry.

The basic equations used to model the film distribution of the multiple sources across the substrate plane are presented along with sample calculation results used to demonstrate the application of the model to the specific experimental deposition configuration that is reported here. This is followed by a description of the deposition chamber configuration and the deposition process parameters. Experimental results are presented and compared to the model predictions. An analysis of the results and conclusions reached are presented in the final sections of this paper.

2. Calculation of film uniformity

2.1 Basic calculations

The distribution of material from a directed surface source is given by[1]

$$dM = \left[\frac{m}{\pi}\right] \cos\varphi \, d\omega \tag{1}$$

where m is the total amount of material generated by the source, dM is the amount of material generated through the solid angle dω, and φ is the angle of dω relative to the normal to the surface of the source. This relation is based on the assumption that the material evolved from the surface source exhibits a cosine distribution.

The right side of Equation 1 can be converted from a differential solid angle to a differential surface area in a plane by the substitution

$$dS = \frac{r^2 \, d\omega}{\cos\theta} \tag{2}$$

where r is the distance from the source to the plane and θ is the angle between the source point and the surface normal of the area of interest. Equation 1 then can be written as

$$dM = \left[\frac{m}{\pi}\right] \frac{1}{r^2} \cos\varphi \cos\theta \, dS. \tag{3}$$

For most practical applications the distribution of material on a plane at a fixed distance above the source and parallel to the source surface is the configuration of greatest interest. The following analysis will be limited to this configuration. For applications concerning distributions on other geometries the surface of interest can be broken into a series of concentric flat rings at differing heights and the same analysis applied as long as the surface is not so steeply curved that it partially shadows the vapor stream from the source. It is also assumed that the substrate plane is rotating about a fixed axis and that axis is perpendicular to the plane containing the source.

The geometry of this configuration is shown in Figure 1 and the surface on which the film is deposited is labeled the substrate plane.

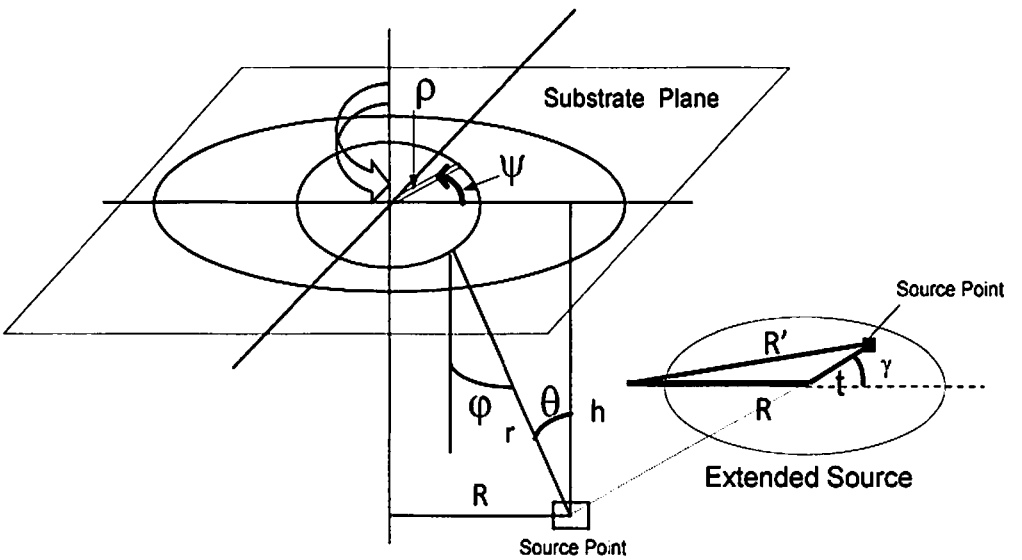

Fig. 1. Schematic of the deposition geometry. For the extended source the single point source is replaced by the set of point sources representing the target area with the appropriate geometry as shown on the right.

The differential surface area in the substrate plane for this geometry can be then written

$$dS = \rho d\psi d\rho, \tag{4}$$

where $\rho d\psi$ is the differential arc length at radius ρ and $d\rho$ is the differential radius. For a substrate plane parallel to the source surface φ=θ and inserting 4 into 3 results in

$$dM = \left[\frac{m}{\pi}\right]\frac{1}{r^2}(\cos\theta)^2 d\rho d\psi. \tag{5}$$

From the geometry of Figure 1

$$\cos\theta = \frac{h}{r} \tag{6}$$

where

$$r = \sqrt{\left(h^2 + (\rho^2 + R^2 - 2\rho R\cos\psi)\right)}, \tag{7}$$

and R is the distance from the origin of the substrate plane coordinate system projected on to the source plane, as shown in Figure 1. Using Equations 6 and 7, Equation 5 can be written as

$$dM = \left[\frac{m}{\pi}\right]\frac{h^2}{(h^2+(\rho^2+R^2-2\rho R\cos\psi))^2}\,\rho d\rho d\psi. \tag{8}$$

Equation 8 can now be integrated across an area of the substrate plane to yield the total amount of material deposited on this area from a point on the source. The solution for an anular region of the substrate plane, results in the equation

$$M = \left[\frac{m}{\pi}\right]\int_0^{2\pi}\int_{\rho_1}^{\rho_2}\frac{h^2}{(h^2+(\rho^2+R^2-2\rho R\cos\psi))^2}\,\rho d\rho d\psi. \quad , \tag{9}$$

where M is the amount of material deposited on the anular area between ρ_1 and ρ_2.

Equation 9 can also be used to find the realtive distribution of the material on the substrate plane. If the substrate plane is rotating relative to the source as indicated in Figure 1 at an angular velocity that is large compared to the rate at which the vapor molecules are arriving at the substrate plane surface, the material will be uniformly distributed azmuthally. If the annular regions correspond to small enough increments, the radial distribution will correspond to the fractional amount of material deposited in the annular area to the total material generated by the source.

2.2 Modifications for extended sources

The above analysis can be used for applications where the dimensions of the source are small compared to the dimensions of the area across which the film uniformity is of interest. The distribution can be normalized to the film thickness at some point on the substrate plane to yield a relative thickness distribution or it can be used to find the ratio M/m which will be useful when the distribution from multiple sources is being calculated.

To calculate the distribution from an extended source Equation 9 must be evaluated across the surface of the source. The geometry of this configuration is shown in the inset to Figure 1. The integration across the source is performed by integrating across the source radius t and angle γ over 2π, thus covering the surface. The distance r from a point on the source to a point on the substrate plane can now be written as

$$r = \sqrt{\left(h^2 + \left(\rho^2 + R'^2 - 2\rho R'\cos\psi\right)\right)} \tag{10}$$

Where

$$R' = \sqrt{(t^2 + R^2 - 2tR\cos\gamma)}. \tag{11}$$

Equation 9 can now be written as

$$M = \left[\frac{m}{\pi}\right] \int_{t_1}^{t_2} \int_0^{2\pi} \int_0^{2\pi} \int_{\rho_1}^{\rho_2} \frac{h^2}{\left(h^2+(\rho^2+R^2-2\rho R'\cos\psi)\right)^2} \rho d\rho d\psi d\gamma dt, \tag{12}$$

where t_1 and t_2 are the inner and outer radius of the source.

A modification to Equation 12 may be required to improve the fit to actual data. The initial assumption of a perfect cosine distribution of the vapor from the source frequently is not true and a cosine distribution to a power other than one must be used. Usually the power is not greatly different from one, but is in the range of 0.7 to 1.3. When this substitution is made Equation 12 becomes

$$M = \left[\frac{m}{\pi}\right] \int_{t_1}^{t_2} \int_0^{2\pi} \int_0^{2\pi} \int_{\rho_1}^{\rho_2} \frac{h^{1-g}}{\left(h^2+(\rho^2+R^2-2\rho R'\cos\psi)\right)^{1.5-g-0.5}} \rho d\rho d\psi d\gamma dt, \tag{13}$$

where g is the power of the cosine. A value of g greater than 1 indicates a vapor stream more directed along the normal to the target and less than 1 a vapor stream more directed parallel to the target. Although Equation 13 was derived for a circular source, the analysis can be applied to any planer source geometry with the appropriate limits of integration and possibly a substitution of a more convenient coordinate system. For all of the modeled distributions presented in this paper the parameter g was set to one, which as the empirical results will show, yielded an adequate fit to the data.

In Equation 13 the fractional power in the denominator of the integrand results from the denominator being a product of the distance-to-the-substrate-plane squared, the cosine of the angle to the substrate plane normal and the cosine of the angle to the source normal (see Equations 3 through 5 and considering that the power of $\cos\varphi$ is not 1). For $g = 1$ the power of the cosine of the angle to the substrate plane normal and the power of the cosine of the angle to the source distribution normal are identical, but for $g \neq 1$ they are not equal.

It is convenient to normalize Equation 13 such that for a substrate plane that extended to infinity the ratio M/m=1, indicating all of the material generate from the deposition source is collected at the substrate plane. The normalization factor is found to be $1/(2\pi(t_2-t_1)\,a)$, where a is given by

$$a = \int_0^{\frac{\pi}{2}} \int_0^{2\pi} \cos(\theta)^g \sin\theta \, d\rho \, d\theta. \tag{14}$$

With this normalization factor the fraction of the material generated by the source that is deposited on an annular region of the substrate plane can be calculated.

Two assumptions are made in these calculations: (1) the vapor pressure generated by each individual target is low enough so material generated by one source does not interfere with material from another source and (2) the distribution from all sources is the linear superposition of the individual sources. The total film distribution is the sum of the normalized distributions for each of the sources, as calculated using Equation 12. When performing the summation the deposition rates for each source are adjusted by a weighting factor if the deposition rates are different.

These calculation are useful for predicting the film distribution for a given substrate geometry and the utilization efficiency of the material generated from a source. Higher utilization of the material increases the deposition rate on the substrate, reduces the amount of material that is deposited on the chamber walls and fixtures and ultimately lowers overall chamber maintenance.

A sample of the input parameters and calculations results for the silicon targets used in these experiments are presented in Table 1 & 2 to illustrate the computational technique. The height (h) is the perpendicular distance from the source surface to the substrate plane where the uniformity was measured and the radius (R) is measured from the axis of rotation of the substrate plane. The relative rate is the calculated rate at which material leaves the source normalized to the rate of

source #1. The calculated efficiency is the ratio of the material deposited on the substrate plane to the total amount of material leaving the source.

Table 1. Si target parameters and calculation results

Source #	Height (h) (cm)	Radius (R) (cm)	Relative Rate	Efficiency
1	52.100	30.500	1.000	0.694
2	52.100	63.500	1.450	0.537
3	44.500	86.400	3.200	0.376

Using Table 1 as the input parameters the distributions of three Si magnetron sources was computed using Equation 13, normalized using Equation 14. For these calculations the power of the cosine function in Equation 13 was set to 1. The results of the distribution calculations are summarized in Table 2. The first column of the table lists the radial limits (ρ_1 and ρ_2) used in the distribution calculation and the second column is the computed annular area between ρ_1 and ρ_2. The distribution, defined as the ratio M/m of the material deposited in each area, is shown in columns 3 though 5, for the three sources.. For example, within the area from the center of the substrate out to a radius of 2.54cm, source #1 deposits 0.13% of the total material leaving its surface; source #2 deposits 0.039% of vapor material; and source #3 deposits 0.014% of its vapor material.

Table 2. Si distribution calculation results.

Annular Radii (cm)	Annular Area (cm^2)	Source 1 Material Ratio ($x10^{-3}$)	Source 2 Material Ratio ($x10^{-3}$)	Source 3 Material Ratio ($x10^{-3}$)	Weighted Sum Material Ratios ($x10^{-3}$)	Material Ratio/Unit Area (cm^{-2}) $x10^{-4}$	Relative Thickness
0.000 - 2.540	20.268	1.313	0.388	0.143	2.332	1.150	0.996
2.540 - 5.080	60.805	3.932	1.168	0.429	6.998	1.151	0.997
5.080 - 7.620	101.341	6.529	1.958	0.721	11.674	1.152	0.997
7.620 - 10.160	141.878	9.087	2.765	1.020	16.360	1.153	0.998
10.160 - 12.700	182.415	11.590	3.596	1.332	21.067	1.155	1.000
12.700 - 15.240	222.951	14.010	4.458	1.659	25.783	1.156	1.001

The weighted sum is defined as the sum of the products of the material ratio from each source with the relative rate for each source. The material/unit area is this weighted sum divided by the annular area. This number can be converted to a film thickness when the total mass, generated from the sources and film material density, is specified. The final column is the material ratio/unit area normalized to one at a specific radius and gives the relative thickness of the film. The radius chosen for this example was 10.16cm because this is the closest point to center of the chamber that actual data could be obtained. The calculations were performed out to 81cm radius, but in the interest of brevity the calculation results for only the first six annular regions are presented here.

3. Deposition system and experimental results

3.1 Deposition system

The vacuum system used for the deposition experiment is a 2.5 meter box coater. The pumping system of the chamber consists of two mechanical pumps with roots blowers and two 81cm diameter diffusion pumps using DC 705 pump fluid. Cryogenic traps are located between the pumps and the chamber to prevent back streaming of the diffusion pump fluid and increase the pumping speed of water vapor. The chamber is crossed over from the roughing to the diffusion pumps at

0.10 Torr (13.3 Pa). The pumping speed of the chamber in high vacuum is 16,000 liters/second for argon. The base pressure of the chamber, prior to the start of deposition, is approximately $2x10^{-7}$ Torr ($3x10^{-5}$ Pa).

The principle components of the deposition system are shown in Figure 3. For these experiments we evaluated single layer film thickness of two different deposition materials: silicon and niobium. For each material we operated three magnetrons simultaneously. The two groups of magnetrons are arranged on opposite sides of the chamber. The magnetrons are number as they are referenced in Table 1. The magnetrons are 20cm diameter and are powered by pulse modulated power supplies. Argon gas flow to each of the magnetron sources is individually controlled with a mass flow controller. This provides improved control of the deposition rate.

An end Hall ion source is located in the chamber to provide energetic oxygen to increase the reaction rate of oxygen with the metal vapor sputtered from the targets. The ion source beam voltage was 100V to 110V depending on the material being sputtered. The end Hall ion source also contains a hollow cathode electron source. In addition to providing a source of energetic oxygen, the ion source acts as a system to supply or absorb electrons, as required, to stabilize the magnetrons. This results in a significant decrease in arcing of the magnetrons. Additional oxygen is brought into the chamber through a single mass flow controller and distributed through a manifold directed toward the substrate. An optical monitor and four crystal mass balance monitors are installed in the chamber to accurately control the film thickness and deposition rates. Witness samples, located in the substrate plane, were used to measure the actual deposited film thickness along the radius of the coating chamber.

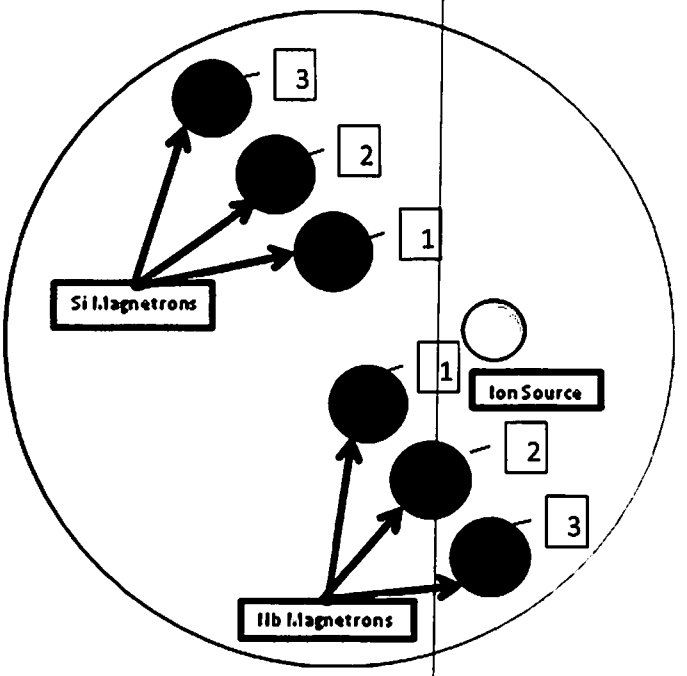

Fig. 2. Coating chamber configuration.

3.2 SiO_2 deposition process and results

Single layer SiO_2 films were deposited using boron doped silicon targets. Three deposition runs were made and results were analyzed. For each of the deposition runs the argon flow rate for each magnetron was 40 sccm. The oxygen was supplied at a flow rate of 120 sccm. The pressure during deposition was $3.9X10^{-4}$ Torr ($5.2X10^{-2}$ Pa).

The voltages, currents and argon flow rate of each silicon target are shown in Table 3. The voltages were experimentally determined, in prior runs, to provide the relative rates shown in Table 1. The total deposition rate resulting from the three magnetrons was 0.14nm sec^{-1}. The ion source beam voltage was 110 V for the first two runs and 130V for the final run. The ion source cathode emission current was 4.2 Amps and the anode current varied from 7.0Amps to 7.7Amps. The flow rate for the ion source was 15 sccm of oxygen.

Table 3. Si magnetron parameters.

Magnetron #	Voltage (V)	Current (Amps)	Argon Gas Flow (sccm)
1	370	4.7	40
2	440	4.8	40
3	650	5.7	40

The experimental properties of interest are the optical properties and distribution of the single layer films that were deposited on witness samples. 2.54cm diameter BK-7 glass substrates were held in an aluminum bar fixture with holes spaced 2.54cm apart along the radius of the substrate plane. For these experiments only 6 holes were populated with substrates. The fixture revolved at 18 rpm and rotated at least 500 times during the deposition to provide sufficient azimuthal symmetry for this investigation. The reflectance and transmittance of the coated substrates were measured using a spectrophotometer. Film thickness and refractive index was calculated from the spectral reflectance and transmittance data using a thin film software package. The real part of the refractive index as a function of wavelength is shown in Figure 3. The imaginary part was below the resolution limit of the spectral measurements ($1X10^{-4}$). These results are consistent with previous investigations of sputtered SiO_2 films.[6,7]

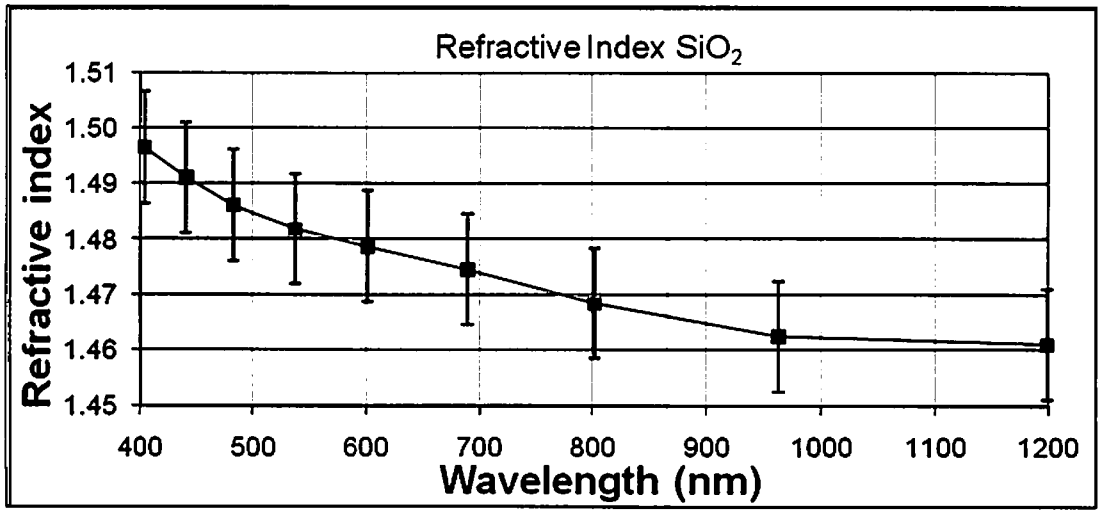

Fig. 3. Refractive index of SiO_2 films.

Figure 4 shows the theoretical distribution of the SiO_2 film based on the model calculation results that were presented in Table 2. The results of three consecutive deposition runs are also shown in Figure 4. The legend shows the symbols associated with the actual empirical data points. The interpolation between measured film thickness is a spline fit used for facilitate visualizing the film thickness if all data points were present. The actual distribution and the model are in good agreement. The distribution of the three deposition runs reproduced closely, demonstrating the process is controllable and repeatable. For each of the three deposition runs the thickness of the coating varied by less than 1% across a radius of 0.68 meters. In addition the thickness distribution of the films remained within 1% when all three films

are considered as an ensemble and no film deviated from the model by more than 1% at any point measured along the radius.

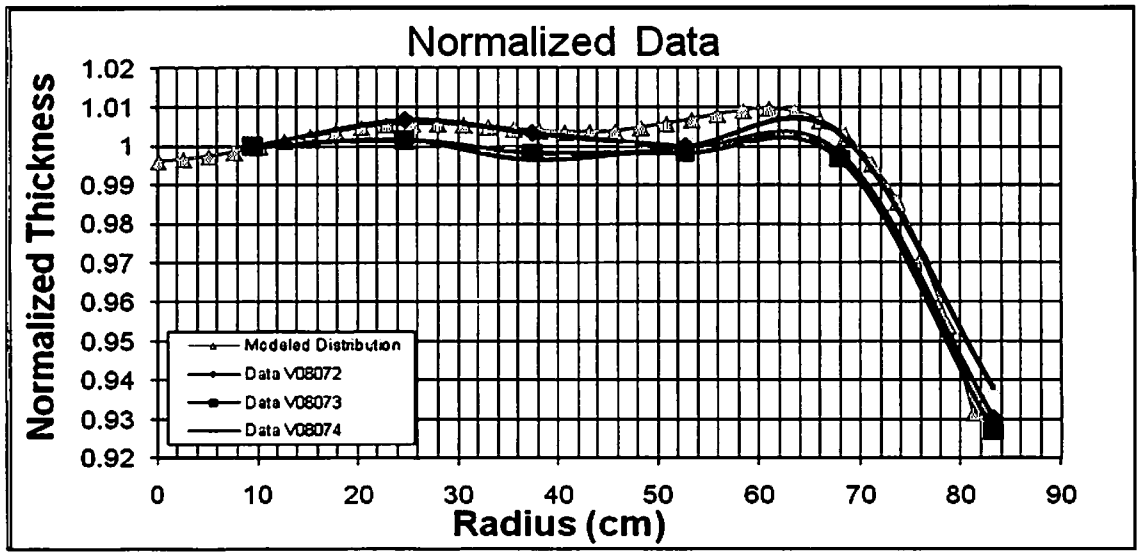

Fig. 4. Distribution of the SiO_2 films.

3.3 Nb_2O_5 deposition process and results

The Nb_2O_5 films were deposited using 99.95% pure niobium targets. The locations, relative rates and efficiency for the niobium magnetron sources are listed in Table 4. As with the silicon magnetron sources, argon gas flow to each of the magnetrons was individually controlled with a mass flow controller. The oxygen was supplied at a flow rate of 50 sccm. The pressure during deposition was $4.0X10^{-4}$ Torr ($5.3X10^{-2}$ Pa).

Table 4. Niobium cathode parameters.

Source	Height (cm)	Radius (cm)	Relative Rate	Efficiency
1	52.100	30.500	1.000	0.657
2	52.100	63.500	1.800	0.510
3	38.700	86.400	2.300	0.382

The voltages, currents and argon flow rate of each niobium magnetron are shown in Table 5. The voltages and flow rates were determined to provide the relative rates shown in Table 4. The total deposition rate resulting from the three magnetrons was 0.08nm sec^{-1}. The ion source beam voltage was 100 V for all depositions. The flow rate for the ion source was 30 sccm of oxygen. The ion source emission current was controlled at 7.5 Amps. The anode current varied from 9.5Amps to 9.8Amps.

Table 5. Nb magnetron parameters.

Magnetron #	Voltage (V)	Current (Amps)	Argon Gas Flow (sccm)
1	550	2.0	45
2	570	2.3	45
3	650	2.8	50

Film distribution, thickness and refractive index were determined using the same method as for the SiO_2 films. The real part of the refractive index of the Nb_2O_5 films as a function of wavelength is shown in Figure 5. The imaginary part of the Nb_2O_5 films was also below the resolution limit of the spectral measurements. Previous investigations of sputtered Nb_2O_5 films have yielded similar refractive indices.[7,8]

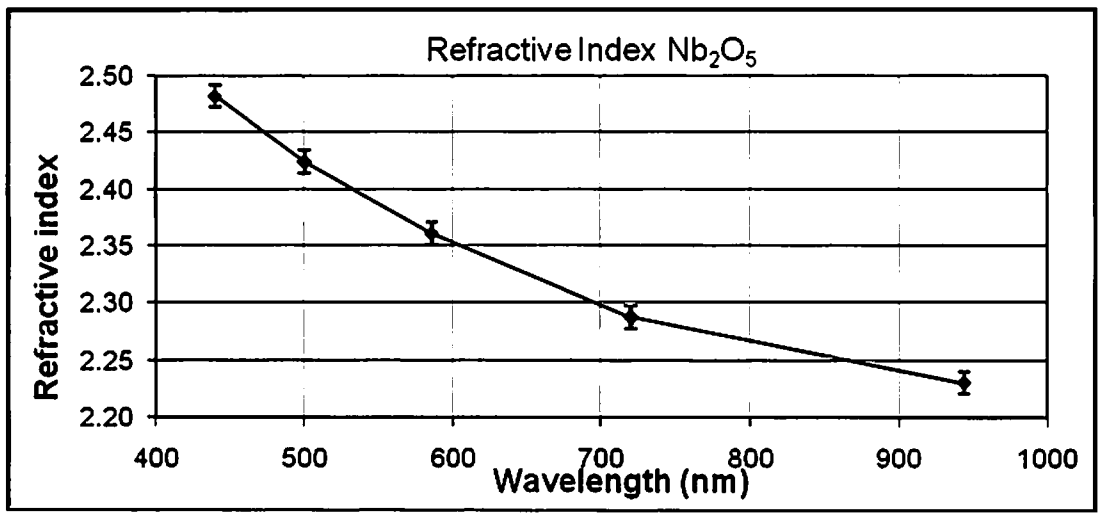

Fig. 5 Refractive index of the Nb_2O_5 films.

Figure 6 shows the modeled distribution of the Nb_2O_5 film and the results of four consecutive actual depositions. The maximum deviation of the distributions of the actual films from the model was 3.3%. The distribution of the four depositions did not reproduce as well as the SiO_2 films. The film that deviated the greatest from the other films, identified as V08115, was deposited at an oxygen flow rate of 45 sccm while the other films were deposited at a flow rate of 50 sccm. There are also kinks in the distribution, such as the one at 20cm radius for V08115, which cannot be explained by the model. For the four depositions the maximum coating variation for any single film was 2.9% across a radius of 0.7 meters. The maximum deviation of any data point from any other data point for all four films was 5%.

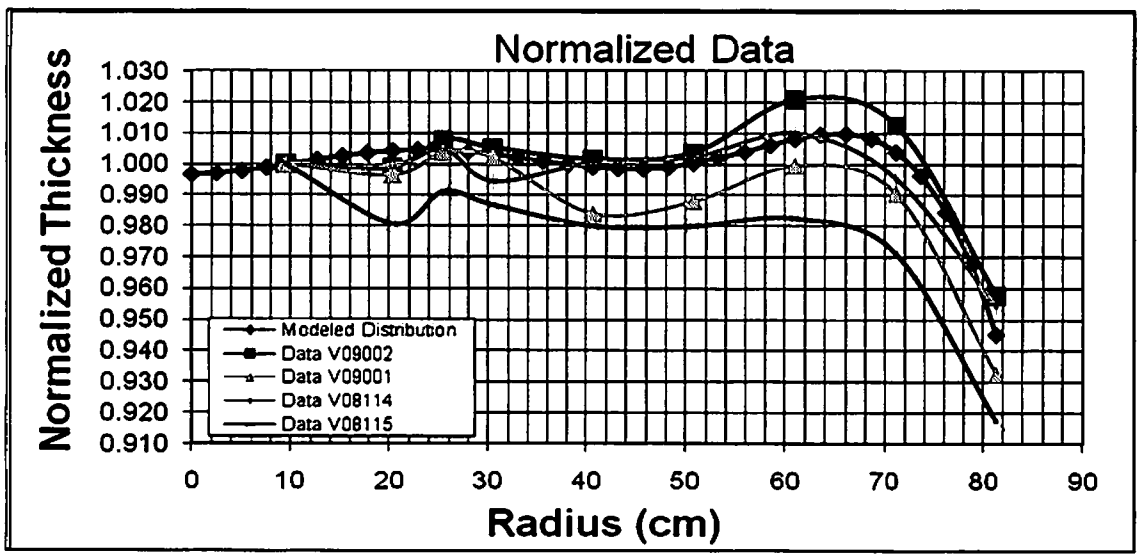

Fig. 6. Distribution of the Nb_2O_5 films.

4. Discussion

The calculations required for modeling the film distribution from multiple sputtering sources have been described above. This model can be used to establish the source configuration and vapor generation rate of multiple sources to achieve a predetermined film distribution. The results of using the model distributions to configure three sources for SiO_2 film deposition resulted in very good agreement with the model. More divergent results were obtained for the Nb_2O_5 films.

A possible cause of divergence of the actual films from the model is reflection of the sputtered molecules from the chamber walls or other objects in the chamber. The model does not include this factor. Another factor is collisions of the vapor stream from one cathode with the vapor stream of an adjacent cathode. The density of the vapor stream near the cathode is sufficient that the mean free path of the molecules is approximately a few centimeters. This would probably be more pronounced for the Nb_2O_5 films because the moment of the Nb_2O_5 molecules is so much greater than the argon or oxygen molecules and only collisions between Nb_2O_5 molecules would significantly alter their trajectory. The momentum of the SiO_2 molecules would be much closer to excited argon and oxygen molecules resulting in a more random scattering of the SiO_2 molecules. This may account for the "kinks" seem in the Nb_2O_5 film distribution. This hypothesis can be tested by locating the sources at larger distances from each other, such as moving the niobium magnetron located at position 2 to the position 2 location of the silicon magnetron, and seeing if the "kinks" disappear.

The model did not take into account the erosion of the targets of the magnetron sources. The targets were approximately 3mm thick and were replaced when the target had less than 0.5mm of material left. Considering the large distances of the source to the substrate relative to the target depth of wear it was assumed this factor would be insignificant from run to run. Each run eroded the target by less than 0.01 cm. As a check the distribution from Si magnetron 2 was calculated at a height of 52.06cm and 52.07cm and compared. It was found that the distribution change by less than 0.1%. Across the life of the target the height would change from 51.82cm to 52.07cm and the distribution would shift by 0.6%. This indicates that this factor needs to be accounted for across the life of the target.

The magnetron source arrangement used in this investigation provides a significant improvement in utilization of the target material compared with a single target of the same dimensions. The total utilization of material with the three sources is 48% of the material generated by the sources deposits on the substrate. For a single round source providing the same uniformity distribution only 14% is deposited on the substrate. This implies that 3.4 times as much material must be generated from the single source for similar film uniformity. For a 6 inch by 24 inch rectangular substrate providing the same distribution uniformity only 12% is deposited on the substrate.

5. Conclusion

The data presented above indicate that the deposition distribution from multiple magnetron sources can be accurately modeled and that a deposition system based on this model produces films with the modeled uniformity. This was demonstrated over a 68cm radius which results in an area of $1.45m^2$ that can be uniformly coated. Some deviations from the model were observed and further investigation into the origin of these deviations is required. For many practical applications the observed deviations are not sufficient to be of concern. Although the model and experimental results were demonstrated only for a planer region, the extension to curved surfaces should pose no difficulties.

Two important advantages are achieved by this deposition process. Uniformity over large areas can be established without the use of uniformity shields by proper positioning of the magnetron sources and vapor generation rate control. This reduces setup time and opportunities for errors. The efficiency of utilization of coating material is improved so that deposition rates can be increased and maintenance is reduced.

References

[1] Macleod, H. A., [Thin Film Optical Filters], Taylor &Frances, New York & London, 488-497 (2001).

[2] Holland, L., and Stecklmacher, W. , "The distribution of thin films condensed on surfaces by the vacuum evaporation method," Vacuum, 11 (4), 346-364 (1953).

[3] Oliver, J. B., "Optimization of deposition uniformity for large-aperture National Ignition Facility substrates in a planetary rotation system," Appl. Optics 45 (13), 3097-3105 (2006).
[4] Swann, S., "Film thickness distribution in magnetron sputtering," Vacuum 38 (8-10), 791-794 (1988).
[5] Swann, S., Collett, S. A., and Scarlett, I. R., "Film thickness distribution control with off-axis circular magnetron sources onto rotating substrate holders: Comparison of computer simulation with practical results," J. Vac. Sci. Technol. A 8 (3), 1299-1303 (1990).
[6] Cheng-Chung Lee and Der-Jun Jan, "DC magnetron sputtering of Si to form SiO_2 in low-energy ion beam," J. Vacuum 80, 693-697 (2006).
[7] Richter, F., Kupfer, H., Schlott, P., Gessner, T. and Kaufmann, C., "Optical properties and mechanical stress in SiO_2/Nb_2O_5 multilayers," Thin Solid FIlms 389, 278-283 (2001).
[8] Gibson, D. R., Brinkler, I. Hall, G. W., Waddell, E. M. and Walls, J. M., "Deposition of multilayer optical coatings using closed field magnetron sputtering," Proc. SPIE 6286, 628601-1-628601-13 (2006).

DISTRIBUTION LIST

DTIC/OCP
8725 John J. Kingman Rd, Suite 0944
Ft Belvoir, VA 22060-6218 1 cy

AFRL/RVIL
Kirtland AFB, NM 87117-5776 2 cy

Stanley Peplinski
Official Record Copy
AFRL/RDSO 1 cy